Proceedings of the 2004 IEEE
International Conference on Robotics & Automation
New Orleans, LA • April 2004

Motion Planning for a Rod-shaped Robot in $\mathbb{R}^3$: Connecting the Rod-HGVG using the Point-HGVG

Ji Yeong Lee and Howie Choset
Department of Mechanical Engineering
Carnegie Mellon University
Pittsburgh, Pennsylvania, USA
jiyeongl@andrew.cmu.edu, choset@cs.cmu.edu

***Abstract*— This work considers the motion planning for a rod-shaped robot in a three-dimensional space. Our approach is to construct a roadmap in the configuration space of the rod and use it to navigate and map unknown spaces. Previously, we defined the rod-HGVG, which is a roadmap for a rod-shaped robot operating in a three-dimensional space. However, the rod-HGVG is only guaranteed to be connected if the point-GVG is connected. This work extends the rod-HGVG into more general environments where the point-GVG may not be connected but the point-HGVG is connected. For this, we define new components, termed the *higher-order edges* for the rod-HGVG and linking strategies which are based on the point-HGVG. Just as there is a close relationship between the components of the point-GVG and the rod-HGVG, there is a close relationship between the components of the point-HGVG and the higher-order edges of the rod-HGVG. We provide the construction procedures for the higher-order edges, which, like the components of the rod-HGVG, can be constructed using only sensor-provided information.**

I. Introduction

This work examines sensor based planning in a non-Euclidean configuration space. Sensor-based planning differs from classical planning in that full knowledge is not available to the robot prior to the planning event. Our approach here is complete, in that there are provable guarantees which ensure the robot has indeed explored the space. This differs from heuristic methods [14] which do not have guarantees and the probabilistic methods [18], [25] which tradeoff full completeness for computational efficiency.

In all of these areas, three motion planning techniques dominate the field: potential functions, roadmaps, and cellular decompositions. Potential function methods [2], [11], [15]–[17] find a path by tracing a vector field defined on the space, but often have problems with local minima. Roadmaps [5], [7] are one-dimensional structures that a robot can use to plan paths between start and goal many times. Since roadmaps possesses the properties of accessibility, connectivity and departibilit, simply constructing the roadmap using sensor data is a kin to exploration because once the roadmap is constructed, the planner can use it for future excursions into the environment. Cellular decomposition methods [4], [22] decompose the free space into simple cells and then represent the relation between cells using an adjacency graph which is used to find a path between the cells.

In this work, we extend the authors' previous work on sensor-based planning for rod-shaped robots in three dimensions [19]. Even though we are mainly interested in rod-shaped robots as a stepping stone towards motion planning of the highly-articulated robots, rod-shaped robots are interesting in themselves because their configuration space is non-Euclidean. The previous work [19] introduced a roadmap for the rod operating in $\mathbb{R}^3$ termed the *rod-hierarchical generalized Voronoi graph* (rod-HGVG) and its incremental construction procedure. The proof of completeness, however, assumed that an $\mathbb{R}^3$ workspace structure, the point-generalized Voronoi graph (point-GVG), was connected. This is not a reasonable assumption since the point-GVG, in general, is not connected in $\mathbb{R}^3$. In this work, we re-define the rod-HGVG without this assumption. We do, however, assume that the *point-hierarchical generalized Voronoi graph* (point-HGVG) – an extension of the point-GVG – is connected. With this assumption, we introduce new components of the rod-HGVG, termed the *higher-order edges*, to connect the disconnected components of the rod-HGVG. We also provide the linking procedures from the higher-order edges to the disconnected components of the rod-HGVG.

One structure of interest, defined in this work, is the *rod-occluding edge*, which arises because we consider more obstacles than the closest ones. Unlike the other components of the rod-HGVG, the rod-occluding edges are defined using the discontinuity of a function, and they cannot be constructed using a root tracing technique used in [8]. We present a new tracing method for the rod-occluding edges using only sensor-provided information.

The organization of this paper is as follows. In Section II, we discuss some of the planning methods based on the generalized Voronoi diagram; in particular we discuss the point-HGVG and the rod-HGVG in $\mathbb{R}^3$ in some detail since this work uses these roadmaps. In Section III, we define the higher-order rod-HGVG edges, and discuss the tracing methods for them. Finally, Section IV summarizes this work and discusses some of the remaining issues.

II. Prior Work

A. GVD-related work

This work belongs in the family of planning methods that use the generalized Voronoi diagram (point-GVD) [1] as their basis. The point-GVD is defined using the Euclidean distance, i.e., the distance between the point x and the obstacle C_i is

defined as

$$d_i(x) = \min_{c \in C_i} \|x - c\|. \quad (1)$$

Then the point-GVD is defined as the union of point-two-equidistant faces F_{ij}, which is the set of points equidistant to obstacles C_i and C_j, i.e., $F_{ij} = \{x \in \mathbb{R}^n : 0 \leq d_i(x) = d_j(x) \leq d_k \forall k \neq i, j\}$.

In the plane, the point-GVD forms a one-dimensional set and Ó'Dúnlaing and Yap [23] first applied the point-GVD to path planning for a disk-shaped robot – which can be modeled as a point – operating in the plane.

The generalized Voronoi graph (point-GVG) is a generalization of the point-GVD and is defined as the set of points equidistant to n obstacles in $\mathbb{R}^n$. Especially, in $\mathbb{R}^3$, the point-GVG is the union of point-GVG edges F_{ijk}, which is the intersection of three point-two-equidistant faces F_{ij}, F_{ik} and F_{jk}. The point-GVG edges intersect at the point-GVG meetpoints F_{ijkl}, which are, by definition, the four-way equidistant points. The point-GVG does not form a connected set in $\mathbb{R}^3$ in general (Fig. 1 (a)), and therefore cannot be used as a roadmap by itself.

The point-GVG has been used for motion planning for the robots with general shape in two- or three-dimensional spaces [6], [12], [14], [20], [21]. Recently there have been hybrid approaches [13], [24], [25] that use a randomized planner along with the point-GVD. These methods, in general, are not provably complete and require full knowledge of the space before the planning.

Choset et. al. [10] developed the planar rod-HGVG which is a roadmap for a rod-shaped robot operating in the plane. The rod-HGVG is defined using the workspace distance. The distance between the configuration q and the obstacle C_i is defined as

$$D_i(q) = \min_{r \in R(q), c \in C_i} \|r - c\|, \quad (2)$$

where $R(q)$ is the workspace volume of the rod at the configuration q.

The rod-HGVG in the plane consists of the rod-GVG edges and the one-tangent edges. The rod-GVG edges are the sets of three-way equidistant configurations and are one-dimensional sets. The rod-GVG edges implicitly define the cellular decomposition of the configuration space, such that a rod-GVG edge is a retract of a cell. Since in general there cannot be a one-dimensional retract of the space with dimension greater than two [3], the union of the rod-GVG edges is not connected. To connect the rod-GVG edges, they use the point-GVG, resulting in the one-tangent edges, which is defined as the set configurations which are doubly equidistant and tangent to the point-GVG edges.

The one-tangent edges and the rod-GVG edges roughly correspond to the point-GVG edges and the point-GVG meetpoints in the plane. Actually, the connectivity of the rod-HGVG can be shown using this correspondence.

B. Point-HGVG and Rod-HGVG in $\mathbb{R}^3$

1) Point-HGVG: Choset et. al. [8], [9] extended the point-GVG into the three-dimensional space, resulting in the point hierarchical Voronoi graph (point-HGVG). As noted above, the point-GVG is, in general, not connected in $\mathbb{R}^3$. To connect the point-GVG, we introduce new structures, termed the *higher-order edges* (Fig. 1 (b)). We consider an individual point-two-equidistant face F_{ij}, and define new structures on it to connect the point-GVG edges which are actually the boundary components of F_{ij}.

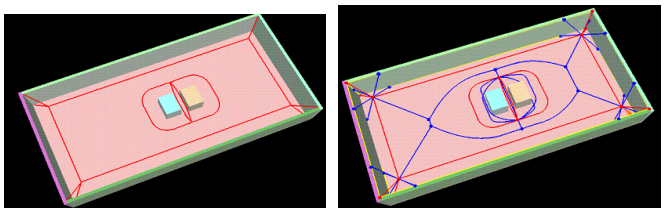

(a) (b)

Fig. 1: The point-HGVG or the hierarchical generalized Voronoi diagram, which consists of the GVG edges and higher-order GVG edges. The GVG in $\mathbb{R}^3$ does not form a roadmap as shown in (a). Using the higher-order GVG edges, disconnected components of GVG can be connected, and thus forming a roadmap (b).

Here we need to consider the obstacles other than the closest ones. For a point x in F_{ij}, the obstacles C_i and C_j are called the *first* closest obstacles and the obstacle which has a distance smaller than other obstacles except C_i and C_j is called the *second* closest obstacle. Since we consider the second closest obstacle as well as the first closest one, we need to pay more careful attention to the definition of the distance function. Let $c_i(x)$ be the closest point on C_i from the point x, i.e., $c_i(x) = \mathrm{argmin}_{c \in C_i} \|x - c\|$. Note that, if there are multiple obstacles, the point $c_i(x)$ may not be "visible" from the point x. That is, the line segment connecting the points x and $c_i(x)$ may not lie completely in the free space. In this case, we define the distance between the point x and C_i to be infinity. This discussion leads us to use the *V-distance function* $d_i^v(x)$, which is defined as

$$d_i^v(x) = \begin{cases} \min_{c \in C_i} \|x - c\| & \text{if } s(x, c_i(x)) \subset FS \\ \infty & \text{otherwise} \end{cases}, \quad (3)$$

where FS is the free space and $s(x, c_i(x))$ is the line segment connecting the points x and $c_i(x)$.

There are three kinds of the higher-order edges in $\mathbb{R}^3$: (i) second-order point-GVG edges, (ii) occluding edges, and (iii) floating boundary edges. The *second-order point-GVG edge* $F_{kl}|_{F_{ij}}$ is the set of point on F_{ij} that contains all of the points equidistant to C_k and C_l. The intersection of two second-order rod-GVG edges is termed the second-order point-GVG meetpoint, denoted by $F_{klm}|_{F_{ij}}$. The second-order point-GVG edges are used to find a disconnected point-GVG cycle, i.e., a point-GVG edge which is homeomorphic to S^1 and is not connected to any other point-GVG edges.

The *occluding edge* arises because of the use of the V-distance function. An occluding edge $V_{kl}|_{F_{ij}}$ is defined as the set of the points on F_{ij} where the distance to the second closest obstacles C_k and C_l changes discontinuously.

The *floating boundary* edge is the set of points on F_{ij}, where

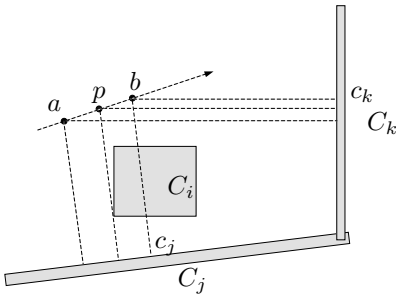

Fig. 2: The closest point on the obstacle C_j from the point b is the point c_j. However, if the line segment connecting x and c_j intersects the first closest obstacle C_i, the distance to the obstacle C_j defined to be infinity for the *V-distance function*. As the robot moves from the point a towards the point b, the second closest obstacle changes from C_j to C_k at the point p, and the distance to the second closest obstacle changes discontinuously.

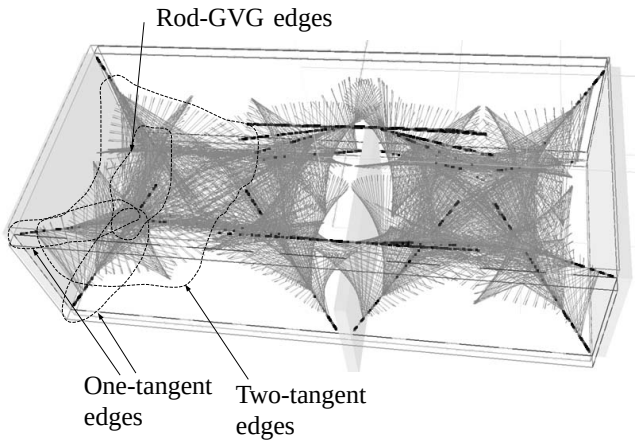

Fig. 3: The rod-HGVG in a rectangular box environment with a block in the middle. The rod-HGVG consists of three components : the rod-GVG edges, the two-tangent edges, and the one-tangent edges.

distance gradients to the two closest obstacles become the same, i.e., $\nabla d_i(x) = \nabla d_j(x)$. The floating boundary edge is required for completeness, but the simulation results from the various environments seem to indicate that the point-HGVG forms a connected set without the floating boundary edges.

Essentially, we are forming a cellular decomposition on F_{ij} (the cells are termed the *second-order generalized Voronoi regions*) and the higher-order edges are the boundary of the cells. Unfortunately, in addition to these components, the point-HGVG also requires some linking strategies since these additional components do not guarantee that the point-HGVG is connected. Instead, these structures give clues about the "directions" to which the planner looks for the disconnected components of the point-HGVG components. A more detailed discussion on this subject can be found in [9].

2) Rod-HGVG in $\mathbb{R}^3$: The rod operating in $\mathbb{R}^3$ has five degrees-of-freedom, i.e., three translational and two rotational degrees-of-freedom, and hence its configuration space is a non-Euclidean five-dimensional space diffeomorphic to $\mathbb{R}^3 \times S^2$.

Just like the planar rod-HGVG, In defining the rod-HGVG in $\mathbb{R}^3$, we form a decomposition of the free space and define a retract, and connect them using *one-tangent edges*. The one-tangent edge is defined as the three-way equidistant configurations tangent to the point-GVG edge in $\mathbb{R}^3$, which can be represented also as

$$\begin{aligned} R_{ijk} &= \{q \in CF_{ijk} : \langle PQ(q), c_i(q) - c_j(q)\rangle = 0 \\ &\quad \text{and } \langle PQ(q), c_i(q) - c_k(q)\rangle = 0\}, \end{aligned} \tag{4}$$

where CF_{ijk} denotes the three-way equidistant configurations, $PQ(q)$ a line segment parallel to the rod at the configuration q, and $c_i(q)$ the closest point on C_i to the rod. The closest point on the rod to C_i is denoted by $r_i(q)$. However, here, the retract is the four-way equidistant-faces CF_{ijkl}, i.e., the set of four-way equidistant configurations, rather than the set of five-way equidistant configurations, even though the rod has five degrees-of-freedom.

The *rod-GVG edges*, which are the sets of the five-way equidistant configurations, i.e.,

$$\begin{aligned} CF_{ijklm} &= CF_{ijkl} \cap CF_{iklm} \cap CF_{jklm}, \\ &\quad \cap CF_{ijkm} \cap CF_{ijlm}, \end{aligned} \tag{5}$$

may not exist at all, and exist only if the rod is long. Then, as in the planar rod-HGVG, one can see the relationships between the point-GVG edge and the one-tangent edge (or rod-GVG edge) and between the point-GVG meetpoint and the four-way equidistant face.

Our retract is the four-way equidistant face, which is two-dimensional, and therefore, we have not defined a roadmap yet. To define a one-dimensional structure, we define another cellular decomposition on the four-way equidistant faces, resulting in the *two-tangent edges*. Two-tangent edges are defined as the set of four-way equidistant configurations that are also tangent to the point-two-equidistant face F_{ij}, i.e.,

$$R_{ij/kl} = \{q \in CF_{ijkl} \ : \ \langle PQ(q), (c_i(q) - c_j(q))\rangle = 0\}. \tag{6}$$

It can be shown that the union of the two-tangent edges (together with the rod-GVG edges if they exist) form a connected set on a four-way equidistant face. From this, it follows that the rod-HGVG – i.e., the union of the rod-GVG edges, the one-tangent edges and the two-tangent edges – forms a connected set (Fig. 3). As in the planar rod-HGVG, in proving the connectivity of the rod-HGVG, we use the connectivity of the point-GVG, which implies that the rod-HGVG may not be connected if the point-GVG is not connected.

III. Main Contribution: Second-order Components of the Rod-HGVG - Connecting the Rod-HGVG using the Point-HGVG

In this section, we define new components of the rod-HGVG, termed *the higher-order edges*, to connect the disconnected components of the rod-HGVG and discuss the construction methods for them. These new structures include (i) second-order one-tangent edges, (ii) second-order rod-GVG edges and (iii) rod-occluding edges.

Since the rod-HGVG is defined using the point-GVG, it is natural to use the point-HGVG to define the components of the rod-HGVG. Just like the higher-order components of the point-HGVG are defined on a two-way equidistant-face F_{ij}, the higher-order components of the rod-HGVG are defined on a two-way equidistant structure. This two-way equidistant structure, denoted by RC_{ij}, is defined as

$$RC_{ij} = \{q \in CF_{ij} \ : \ \langle c_i(q) - c_j(q), PQ(q)\rangle = 0\} \quad (7)$$

The RC_{ij} is three-dimensional, as shown in [19]. Essentially, RC_{ij} is the set of two-way equidistant configurations that are also tangent to the point-two-equidistant face F_{ij}. Note that a two-tangent edge $R_{ij/kl}$ can be defined as the subset of RC_{ij}, i.e., $R_{ij/kl}$ is the set of the configurations in RC_{ij}, which are also four-way equidistant. Also, a one-tangent edge R_{ijk} can be viewed as the intersection of RC_{ij} and RC_{jk}. This gives a motivation to define the higher-order rod-HGVG structures on RC_{ij}, since we want the higher-order rod-HGVG structures to connect the disconnected components of the rod-HGVG. Just like the second-order point-GVG edges result in a planar GVD-like structure defined on the two-dimensional point-two-equidistant face F_{ij}, the second-order edges of the rod-HGVG result in a planar rod-HGVG like structure defined on the three-dimensional RC_{ij}. The rod-occluding edges are also defined on RC_{ij}, and allow the planner to find the disconnected component of the rod-HGVG which is not "visible" from the current configuration.

Before we define the new components of the rod-HGVG, we briefly mention that if there is a point-GVG cycle, there also can be a one-tangent edge cycle, i.e., a one-tangent edge that is homeomorphic to S^1 and disconnected from any other components of the rod-HGVG. Then, from the continuity of the distance function, the one-tangent edge cycle has an even number of local maxima and local minima of the distance along it. This is a different situation from [19], where a one-tangent edge can have at most one local minimum of the distance on it and no local maxima. At the local minima of the distance the rod can slide forwards along the length of the rod at the contact point between the rod and the point-GVG, as described in [19]. At the local maxima, the rod also slides along the length of the rod, but here, it moves backwards until the contact point changes from the one endpoint to the other, and then tracks the point-GVG.

A. Second-order One-tangent Edges

The *second-order one-tangent edges* is analogous to the second-order point-GVG edge, or, as its name suggests, analogous to the one-tangent edge of the planar rod-HGVG. This structure is not necessarily connected to the disconnected components of the rod-HGVG, but provides a "bridge" from which a link can be made to the disconnected components of the rod-HGVG.

The second-order one-tangent edges are defined as follows:

$$\begin{aligned} R_{kl}|_{RC_{ij}} \quad = \quad & \{q \in RC_{ij} : (\mathrm{i}) D_k(q) = D_l(q), \\ & (\mathrm{ii}) \nabla D_k(q) \neq \nabla D_l(q), \\ & (\mathrm{iii}) \langle c_k(q) - c_l(q), PQ(q)\rangle = 0\}. \end{aligned} \quad (8)$$

Essentially, the second-order one-tangent edge traces the second-order point-GVG edge $F_{kl}|_{F_{ij}}$. Since $F_{kl}|_{F_{ij}}$ is the intersection of F_{ij} and SS_{kl}[1], and the rod must be tangent to both of these planes to be an element of $R_{kl}|_{RC_{ij}}$, it follows that $r_i(q) = r_j(q) = r_k(q) = r_l(q)$ for all of the rod configurations in $R_{kl}|_{RC_{ij}}$.

The boundary components, i.e., the endpoints, of the second-order one-tangent edge are either: (i) a boundary configuration (i.e., the distance to the closest obstacles becomes zero), (ii) a four-way equidistant configuration, i.e., a configuration on CF_{ijkl} or (iii) three-way equidistant to the second closest obstacles,. i.e., a configuration q where $D_i(q) = D_j(q) < D_k(q) = D_l(q) = D_m(q)$ for an obstacle C_m (we call this configuration the *second-order connect-configuration*), or (iv) a configuration on an occluding edge.

When the rod reaches a boundary configuration, it simply stops tracing the edge, and returns to the previous node with explored edges associated with it. When the rod reaches a four-way equidistant configuration, the rod is actually at a configuration in a two-tangent edge $R_{ij/kl}$, since the rod is at a configuration in RC_{ij}. Moreover, since $r_k(q) = r_l(q)$ at q, this is a configuration on $R_{kl/ij}$ as well[2]. If the rod reaches a configuration at which it is three-way equidistant to the second closest obstacles, as well as doubly equidistant to the first closest obstacles, then it is on a second-order rod-GVG edge, which is defined in the next section. The case of the occluding edge is discussed in more detail below.

Fig. 4 shows an example of the second-order one-tangent edges in a rectangular enclosure with a box inside. Just like the one-tangent edges of the planar rod-HGVG does not form a connected set by themselves, the union of the second-order one-tangent edges does not form a connected set, even on a single RC_{ij}.

B. Second-order Rod-GVG Edges

The second-order rod-GVG edge is analogous to second-order point-GVG meetpoint, or to the rod-GVG edge for the planar rod-HGVG. Just like the rod-GVG edges connect the endpoints of the one-tangent edges for the planar rod-HGVG, the second-order rod-GVG edges connect the endpoints of the second-order one-tangent edges on RC_{ij}. The second-order rod-GVG edge is defined as

$$\begin{aligned} CF_{klm}|_{RC_{ij}} = \{q \in RC_{ij} \ : \ & (\mathrm{i}) D_k(q) = D_l(q) = D_m(q), \\ & (\mathrm{ii}) \nabla D_k(q) \neq \nabla D_l(q), \nabla D_l(q) \neq \nabla D_m(q), \\ & \nabla D_k(q) \neq \nabla D_m(q)\}. \end{aligned} \quad (9)$$

If the rod were small, $CF_{klm}|_{RC_{ij}}$ would be homeomorphic to S^1, and there would be three second-order one-tangent edges emanating from it. If the rod were long, $CF_{klm}|_{RC_{ij}}$ would be homeomorphic to the union of the closed intervals of $\mathbb{R}$. In this case, the boundary components of $CF_{klm}|_{RC_{ij}}$ are either: (i) a configuration on a rod-GVG edge CF_{ijklm}, (ii) a configuration on an occluding edge, or (iii) a configuration that has the same

[1] $SS_{kl} = \{p \in \mathbb{R}^3 : 0 < d_k(p) = d_l(p), \nabla d_k(p) \neq \nabla d_l(p)\}$

[2] Note that this does not mean this configuration is on a one-tangent edge, since there is no guarantee that $\langle c_i - c_l, PQ(q)\rangle = 0$ at q.

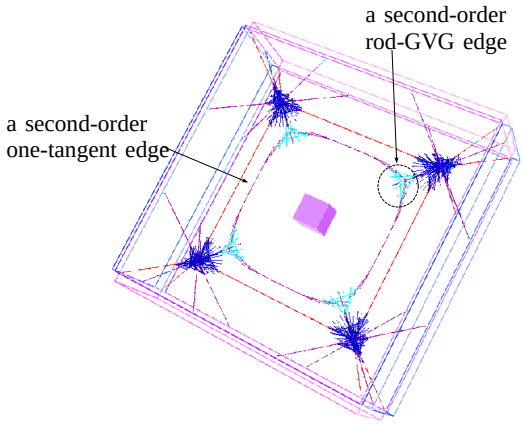

Fig. 4: The rod-HGVG with the second-order edges without the links. Note that there is a point-GVG edge (not shown) associated with the small box, the ceiling and the floor, and hence the one-tangent edge associated with the same set of obstacles. Without linking, just like the point GVG-cycle is disconnected from the other components of the point-HGVG the one-tangent edge associated with the small box is disconnected from the rod-HGVG, even after the second-order edges are constructed.

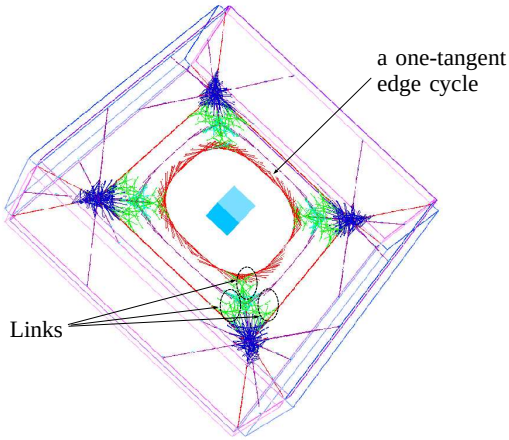

Fig. 5: The rod-HGVG in the same environment as Fig. 4, but with the links. Using the links, the planner can access and trace the inner one-tangent edge cycle. There are links from each of the configurations where a second-order one-tangent edge and a second-order rod-GVG edge intersect each other.

distance to the four second closest obstacles (we term this the *second-order rod-GVG meet-configuration*).

In Fig. 4, we can see that the second-order rod-GVG edges connect the second-order one-tangent edges that lie on the point-two-way equidistant face defined by the top and bottom walls.

C. Connecting to a One-tangent Edge Cycle

Like the second-order point-GVG edges, the second-order one-tangent edges and the second-order rod-GVG edges do not actually connect two disconnected components of the rod-HGVG. Rather, from their structures, the planner can infer that there is a disconnected component of the rod-HGVG and make a connection to it. Here we describe how to make this connection.

For the point-HGVG, the existence of a set of the second-order point-GVG edges whose union is homeomorphic to S^1, indicates that there could be a disconnected point-GVG cycle, i.e., a point-GVG edge that is homeomorphic to S^1 and disconnected from any other components of the point-GVG. [9]. The planner accesses a disconnected point-GVG cycle using a gradient ascent restricted to F_{ij} from the second-point GVG meetpoints. In practice, it is computationally expensive to find a cycle in the point-GVG graph. Instead, the planner attempts to link to a point-GVG cycle at every second-order point-GVG meetpoints. This means that some redundant links are formed in the graph, while the time to search cycles is saved.

Now, note that if there is a point-GVG cycle, there can also be a one-tangent edge cycle, i.e., a one-tangent edge that is homeomorphic to S^1 and disconnected from any other components of the rod-HGVG. Just like the point-GVG cycle can be linked from the second-order point-GVG meetpoint, the one-tangent edge cycle can be linked from the second-order rod-GVG edge since the second-order rod-GVG edge is analogous to the second-order point-GVG meetpoint. Here, as in the point-HGVG, we will try to connect to a one-tangent edge cycle from every second-order rod-GVG edge. Again, this will create some redundant links, while the time to search cycles is saved.

Since the second-order rod-GVG edge is a one-dimensional structure rather than a zero-dimensional structure, we need to choose specific configurations at which the connecting procedure starts. The natural choice would be the configurations where a second-order rod-GVG edge and a second-order one-tangent edge intersect each other, since they are the nodes of the rod-HGVG.

The linking is achieved in two steps. From a configuration $q \in CF_{klm}|_{RC_{ij}} \cap R_{kl}|_{RC_{ij}}$, the rod performs a gradient descent to C_k, while staying on RC_{ij}, until it becomes three-way equidistant to C_i, C_j and C_k. The rod is guaranteed to terminate on a three-way equidistant configuration from the continuity of the distance function. Let this three-way equidistant configuration be denoted by q'. From q' the rod aligns itself to the point-GVG edge defined by C_i, C_j and C_k by following the solution of the curve

$$\dot{c}(t) = \pi_{CF_{ijk} \cap RC_{ij}} v(c(t))$$

where π is a projection operator and $v(q)$ is defined as $v(q) = \left(\pi_{F_{ij}}\left(-\nabla d_k\left(r_i(q)\right)\right), 0\right)$. In a sense, we move the contact point between the rod and F_{ij} towards the point-GVG edge F_{ijk} while keeping the rod on $CF_{ijk} \cap RC_{ij}$. Figs. 5 and 6 show the same environment as in Fig. 4, but with the links to the inner one-tangent edge cycle constructed. Also note that there are some redundant links.

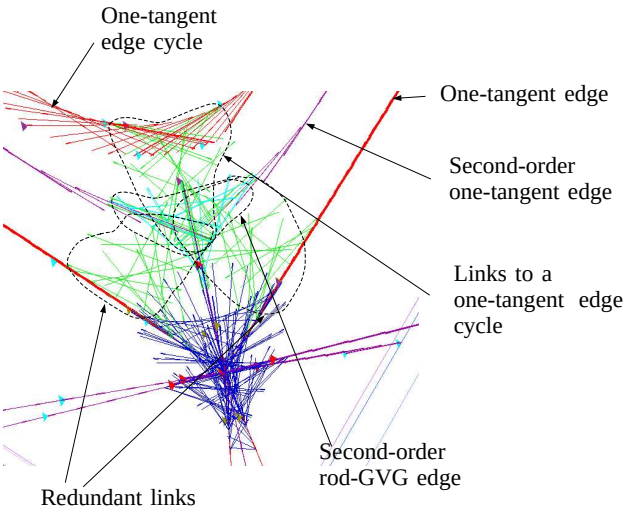

Fig. 6: This figure is the part of the rod-HGVG in the environment shown in Fig. 5 to illustrate, in more detail, the links from the second-order connecting configurations to the inner one-tangent edge cycle. Note also that there are redundant links to the one-tangent edges which do not form a cycle.

D. Rod-Occluding Edges

The point-occluding edge for the point-HGVG is the set of points on F_{ij} where there is a discontinuity in the distance to the second closest obstacle. The motivation for accessing and tracing the point-occluding edge is to look for the point-HGVG components that are not visible from the "current" point-HGVG component. It is assumed that these invisible point-HGVG components are connected to the point-occluding edge, and thus by tracing the point-occluding edge, the planner can access and start tracing the disconnected point-HGVG components. Recall that the components of the point-HGVG are the boundary components of the second-order Voronoi regions, which is defined on an individual F_{ij}, and thus if the point-occluding edge is not an isolated component of the point-HGVG, it must intersect some other components of the point-HGVG.

We could define the rod-occluding edge as the set of configurations where the distance to the second closest obstacle changes discontinuously, which is analogous to the definition of the point-occluding edge. This, in turn, would imply that the rod-occluding edge is a boundary component of the second-order generalized Voronoi region (which could be defined on the rod-two-way equidistant face CF_{ij}, i.e., the set of double equidistant configurations) in the configuration space. However, it should be noted that the other components of the rod-HGVG are not necessarily the boundary components of the Voronoi region or any higher-order Voronoi region, which could be defined recursively on the boundary of the Voronoi region. Thus, there is no guarantee that the rod-occluding edge defined as the boundary component of the second-order generalized Voronoi region intersects any other components of the rod-HGVG.

Instead, we define the rod-occluding edge in such a way that the rod "traces" or "tracks" the point-occluding edge. By tracing, we mean that a rod-occluding edge $RV_{kl}|_{RC_{ij}}$ is defined such that the equation

$$V_{kl}|_{F_{ij}} = \cup_{q \in RV_{kl}|_{RC_{ij}}} r_i(q) \tag{10}$$

is satisfied, where $V_{kl}|_{F_{ij}}$ is a point-occluding edge. This implies that for any point x in $V_{kl}|_{F_{ij}}$, there is a rod configuration q in $RV_{kl}|_{CF_{ij}}$ such that $r_i(q) = r_j(q) = x$. Now, assume that a second-order point-GVG edge $F_{ij}|_{F_{lm}}$ intersects the point-occluding edge $V_{kl}|_{F_{ij}}$ at a point x'. Then, if Eq. 10 is satisfied, there is a configuration $q' \in RV_{kl}|_{RC_{ij}}$, such that $r_i(q') = r_j(q') = V_{kl}|_{F_{ij}} \cap F_{ij}|_{F_{lm}}$. The configuration q' is not necessarily an element of the second-order one-tangent edge $R_{kl}|_{RC_{ij}}$ since q' may not be equidistant to C_k and C_l. However, from q', we could reach a configuration on $RV_{kl}|_{RC_{ij}}$ by sliding and rotating the rod around the point $x' = V_{kl}|_{F_{ij}} \cap F_{ij}|_{F_{lm}}$, which is not difficult since the rod is already in the tangent space of F_{ij} (because the rod-occluding edge is defined on RC_{ij}) and from the point $r_i(q)$, the tangent direction of $F_{ij}|_{F_{lm}}$ can be readily computed. Similar statements can be made about the point-GVG edge intersecting the point-occluding edge and the one-tangent edge associated with it. This means that if a point-HGVG component is connected to the point-occluding edge, the rod-HGVG structure associated with that point-HGVG component can also be easily detected and reached from $RV_{kl}|_{RC_{ij}}$.

With this in mind, we define the rod-occluding edge as follows:

$$\begin{aligned} RV_{kl}|_{RC_{ij}} \quad = \quad & \{q \in RC_{ij} : r_i(q) \in V_{kl}|_{F_{ij}} \text{ and} \\ & R(q) \text{ normal to } V_{kl}|_{F_{ij}}\} \end{aligned} \tag{11}$$

The second condition, i.e., the condition that $R(q)$ is normal to the point-occluding edge, is in some sense arbitrary, and the rod-occluding edge can be defined in different ways as long as it satisfies Eq. 10. We use this definition because, from the simulation results of the point-HGVG in various workspaces, it is observed that, quite often, but not always, the point-HGVG components intersect the point-occluding edge at an angle of $\pi/2$. Thus this definition of the rod-occluding edge could make it easier to connect the rod-occluding edge and the rod-HGVG components that intersect the rod-occluding edge.

The rod-occluding edge can be accessed from a configuration in the one-tangent edge through a gradient descent restricted to RC_{ij}. The planner starts the linking procedure on the configuration in the one-tangent edge where the distance to the closest obstacles attains a local minima. The planner terminates tracing the rod-occluding edge when (i) a rod-occluding edge cycle is detected, (ii) the rod-occluding edge intersects another rod-occluding edge. Recall that for the point-HGVG, it was not possible to determine the tangent direction of the point-occluding edge precisely, and the planner in fact traces the point-occluding edge in a zigzag manner. We can assume that a similar kind of phenomenon would happen in the case of rod-occluding edges defined using the rod-distance function. Then, it would not be easy to determine when the rod should terminate tracing an occluding edge cycle, because it is not generally possible to align the rod precisely along the point-occluding edge. However, with this definition, the rod

can terminate tracing the occluding-edge when the point r_i(q) become sufficiently close to the point $r_i(q_s)$ of the starting configuration q_s, even if there is some error in the orientation.

E. Tracing the Rod-occluding Edge

The second-order one-tangent edges and the second-order rod-GVG edges can be constructed exactly the same way as the rod-HGVG edges are constructed, described in [19]. However, we cannot construct the rod-occluding edge using the same technique, since the rod-occluding edge is defined using the discontinuity of a function.

Recall that even for the point-HGVG, it is not possible to trace the point-occluding edge precisely since the planner cannot determine the precise tangent direction of the occluding edge. Likewise, we cannot expect the planner to trace the rod-occluding edge precisely either. Therefore we present an approximate method to trace the rod-occluding edges.

First we make some observations. We define the *point-occluding face* V_{kl} as the set of points in the free workspace, where the distance to the second closest obstacle changes discontinuously. Then the point-occluding edge $V_{kl}|_{F_{ij}}$ can be defined as the intersection of V_{kl} and F_{ij}. Here, we assume that given a rod configuration q (not necessarily on a rod-occluding edge), if $R(q)$ intersects V_{kl}, we can find the point of the intersection, denoted $o_{kl}(q)$. We also assume that we can find the point $c_k(o_{kl}(q))$, i.e., the closest point on the obstacle C_k from the point $o_{kl}(q)$. Since we assume that we have a series of the range-sensors along the length of the rod, it will not be difficult in practice to find the point where the distance to the second-closest obstacle changes discontinuously. Then, by definition of the point-occluding face, the line passing through $o_{kl}(q)$ and $c_k(o_{kl}(q))$, denoted by $l^{kl}_{occ}(q)$, is tangent to the boundary of the obstacle C_i (assuming, without loss of generality, C_i occludes C_k), and also lies on V_{kl}. This means that there is a plane $T^{kl}_{occ}(q)$ tangent to V_{kl} along $l^{kl}_{occ}(q)$. Finally, if we consider the plane $N^{kl}_{occ}(q)$ that intersects $T^{kl}_{occ}(q)$ at l^{kl}_{occ} and is normal to $T^{kl}_{occ}(q)$, it is not difficult to see that $N^{kl}_{occ}(q)$ is also normal to V_{kl}, and more specifically, $N^{kl}_{occ}(q)$ is normal to $V_{kl}|_{F_{ij}}$ at the point $p = V_{kl}|_{F_{ij}} \cap N^{kl}_{occ}(q)$. This means that a configuration q' such that $R(q') \subset N^{kl}_{occ}(q)$, can easily access the rod-occluding edge by sliding on $N^{kl}_{occ}(q)$.

Now we describe a tracing method for the rod-occluding edge, which consists of two steps : (i) a prediction step and (ii) a correcting step.

The prediction step from a rod configuration q on the occluding edge $RV_{kl}|_{RC_{ij}}$, is a translation of the rod on $T_{r_i(q)}F_{ij}$ (i.e., the plane tangent to F_{ij} at $r_i(q)$), in a direction normal to the vector $PQ(q)$. After the prediction step, the rod would not be on the rod-occluding edge in general. More specifically, the rod might not be on RC_{ij}, and even if it is on RC_{ij}, it might not be normal to the point-occluding edge.

Let q' be the configuration after the prediction step. The correction step works in two steps. First it brings the rod onto $N^{kl}_{occ}(q')$, i.e., after the first correcting step, $R(q') \subset N^{kl}_{occ}(q')$. Then while keeping the rod on $N^{kl}_{occ}(q')$, the second correction step brings the rod back on a configuration in RC_{ij}, which according to the discussion above, is an element of $RV_{kl}|_{RC_{ij}}$ also.

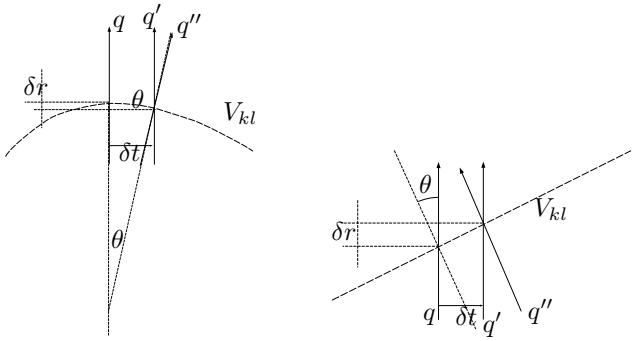

Fig. 7: First correction step: After making a prediction step by translating by δt (from q to q'), the rod is in general not normal either to the occluding edge nor the occluding face V_{kl}. Left: The curved occluding edge: If δt is small so that the occluding edge can be approximated by a circle, we have $\theta = \tan^{-1}(\delta t/\delta o_{kl})$. Right: The initial angle between the rod and the occluding is not $\pi/2$. The correcting θ is computed by $\theta = \tan^{-1}(\delta t/\delta o_{kl})$, where δo_{kl} is the change of the o_{kl} on the rod. Note that we have the same equation for both cases, and can make a correction by rotating the rod by θ, resulting in the configuration q''.

The first step can be done as follows. Assume that initially, the angle between $R(q)$ and $V_{kl}|_{F_{ij}}$ was $\pi/2 + \theta$. Then as shown in Fig. 7, unless $\theta = 0$, the point $o_{kl}(q)$ changes its location on the rod, and we can approximately compute the correcting term as $\theta = \tan^{-1}(\delta t/\delta o_{kl})$, where δt is the translational step size and δo_{kl} is the change in $o_{kl}(q)$ on the rod. Then by rotating the rod by θ around $o_{kl}(q)$ on the plane defined by $PQ(q)$ and $PQ(q')$, we can bring the rod on the $N^{kl}_{occ}(q')$.

Let q'' denote the configuration after the first correction. In general q'' will not be an element of the rod-occluding edge yet and we need a second correcting step that brings the rod onto RC_{ij}. For this, the rod performs a gradient descent of the function $\{D_i - D_j, \langle PQ, c_i - c_j\rangle\}(q)$, while keeping the rod on the plane $N^{kl}_{occ}(q)$, which can be computed using the vectors $PQ(q)$ and $c_i(q) - o_{kl}(q)$ (Fig. 8).

This is the description of the tracing methods for the rod-occluding edge. Note that for the first correction step, we assume that after taking a prediction step, the rod still intersects the point-occluding face. But, since the point-occluding edge and the point-occluding face can have sharp corners, it is possible that the rod may not intersect the point-occluding face after the prediction step. Also, if initially the rod is tangent to the point-occluding edge, the rod will not intersect the point-occluding face after the prediction step. Our current work involves development of additional methods to solve these problems.

IV. CONCLUSION

This work considered sensor-based planning of a rod-shaped robot in a three-dimensional space. This work introduced the higher-order edges for the rod-HGVG, so that the rod-HGVG is connected in more general environments. These structure includes the second-order rod-GVG edge, the second-order one-tangent edge and the rod-occluding edge. These components

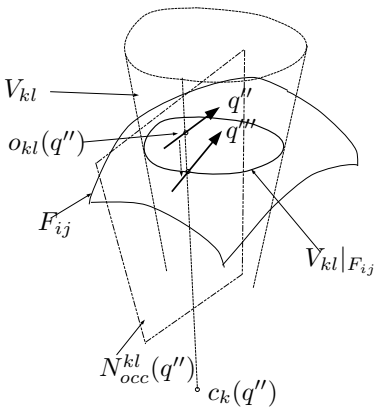

Fig. 8: Second correction step - correcting onto RC_{ij}: From the configuration q'', the rod corrects to q''' which is in RC_{ij} by gradient descent. During this correction, the rod maintains tangency to the plane $N^{kl}_{occ}(q'')$.

are, like the rod-HGVG, defined using the workspace distance, and based on the point-HGVG, a structure in the workspace. More specifically, just as there is a close relationship between the components of the point-GVG and the rod-HGVG, there is a close relationship between the components of the point-HGVG and the higher-order rod-HGVG edges. This relationship essentially guarantees that the rod-HGVG together with the higher-order rod-HGVG edges is connected if the point-HGVG is connected. Since the point-HGVG represents the connectivity of the workspace, the rod-HGVG together with the higher-order edges, in some sense, let us infer the connectivity of the configuration space using the connectivity of the workspace.

However, the rod-HGVG may not be connected even with the higher-order edges in a connected configuration space. As discussed in [9], the linking strategy used for the point-HGVG does not actually guarantee that all of the disconnected components of the point-GVG are connected. Actually an example can be constructed where the point-HGVG is not connected. To completely connect all the point-GVG components would require an exhaustive search on some of the two-way equidistant faces. Since the higher-order rod-HGVG edges are defined using the point-HGVG, the rod-HGVG inherits this problem.

Also, the tracing method for the rod-occluding edge is approximate. However, the advantage of this method is that we use *minimal* information to trace the rod-occluding edge. To trace the rod-occluding edge, we used only the point on the rod where the distance to the second-closest obstacle changes discontinuously. In reality, we could be provided with more information since we assume that there is a series of range sensors along the length of the rod, and using them, we can find more precisely the tangent direction of the point-occluding edge, and thus making tracing procedure for the rod-occluding edge more precise. The next goal of this research is to develop a method that can trace the rod-occluding edge more precisely using more information which is already available from the current sensor model.

REFERENCES

[1] F. Aurenhammer. Voronoi Diagrams — A Survey of a Fundamental Geometric Structure. *ACM Computing Surveys*, 23:345–405, 1991.

[2] J. Borenstien and Y. Koren. Real-Time Obstacle Aviodance for Fast Mobile Robots. *IEEE Transactions on Systems, Man and Cybernetics*, 19(5):1179–1187, 1998.

[3] G. Bredon. *Topology and Geometry, 3rd ed.* Springer-Verlag, 1995.

[4] R. A. Brooks and T. Lozano-Pérez. A subdivision algorithm in configuration space for Findpath with rotation. In *Proceedings of the International Joint Conference on Artificial Intelligence, Karlsrche, Germany*, pages 799–806, Los Altos, Calif., August 1983. William Kauffmann, Inc.

[5] J.F. Canny. *The Complexity of Robot Motion Planning*. MIT Press, Cambridge, MA, 1988.

[6] J.F. Canny and B. Donald. Simplified voronoi diagrams. Technical Report AI Memo No. 957, MIT AI Lab, 1987.

[7] J.F. Canny and M. Lin. An opportunistic global path planner. *Algorithmica*, 10:102–120, 1993.

[8] H. Choset and J. Burdick. Sensor Based Motion Planning: Incremental Construction of the Hierarchical Generalized Voronoi Graph. *International Journal of Robotics Research*, 19(2):126–148, February 2000.

[9] H. Choset and J. Burdick. Sensor Based Motion Planning: The Hierarchical Generalized Voronoi Graph. *International Journal of Robotics Research*, 19(2):96–125, February 2000.

[10] H. Choset and J. Y. Lee. Sensor-Based Construction of a Retract-Like Structure for a Planar Rod Robot. *IEEE Transaction of Robotics and Automation*, 17(4):435–449, August 2001.

[11] J. H. Chuang and N. Ahuja. An Analytically Tractable Potential Fidel Model of Free Space and Its Application in Obstacle Avoidance. *IEEE Transactions on Systems, Man and Cybernetics - Part B: Cybernetics*, 28(5):729–736, 1998.

[12] Abhi Dattasharma and S. Sathiya Keerthi. An augmented Voronoi roadmap for 3D translational motion planning for a convex polyhedron moving amidst convex polyhedral obstacles. *Theoretical Computer Science*, 140(2):205–230, April 1995.

[13] M. Foskey, M. Garber, M. Lin, and Monocha D. A Voronoi-Based Hybrid Motion Planner for Rigid Bodies. Technical Report TR00-025, UNC Chapel Hill Computer Science, 2000.

[14] S.S. Keerthi, C.J. Ong, E. Huang, and E.G. Gilbert. Equidistance diagram- A new roadmap for path planning. In *Proceedings of the IEEE Conference on Robotics and Automation*, pages 682–687, May 2000.

[15] O. Khatib. Real-time obstacle avoidance for manipulators and mobile robots. *International Journal of Robotics Research*, 5:90–98, 1896.

[16] P. Khosla and R. Volpe. Superquadric Artificial Potential for Obstacle Avoidance and Approach. In *Proceedings of IEEE Conference on Robotics and Automation*, pages 1778–1784, 1988.

[17] Y. Koren and J. Borenstein. Potential field methods and their inherent limitations for mobile robot navigation. In *Proceedings of IEEE Conference on Robotics and Automation*, pages 1398–1404, 1991.

[18] Jean-Claude Latombe, Lydia E. Kavraki, Peter Svestka, and Mark Overmars. Probablistic roadmaps for path planning in high dimensional configuration spaces. *IEEE Transactions on Robotics and Automation*, 12(4):566–580, 1996.

[19] J.Y. Lee, H. Choset, and Alfred A. Rizzi. Sensor Based Planning for Rod Shaped Robots in Three Dimensions: Piece-wise Retracts of $\mathbb{R}^3 \times S^2$. In *Proceedings of IEEE International Conference on Robotics and Automation*, pages 991 –999, May 2001.

[20] D. Levin and M. Sharir. Planning a purely translationl motion for a convex object in two dimensional space using the generalized Voronoi diagram. *Discrete and Computational Geometry*, 2:9–31, 1987.

[21] Van-Duc Nguyen. The find-path problem in the plane. Technical Report AI Memo No. 760, MIT AI Lab, 1984.

[22] H. Noborio, T. Haniwa, and S. Arimoto. A feasible motion planning algorithm for a mobile robot on a quadtree representation. In *Proceedings of IEEE International Conference on Robotics and Automation*, pages 327–332, New York, May 1989. IEEE.

[23] C. Ó'Dúnlaing and C.K. Yap. A "Retraction" Method for Planning the Motion of a Disc. *Journal of Algorithms*, 6:104–111, 1985.

[24] Steven A. Wilmarth, Nancy M. Amato, and Peter F. Stiller. MaPRM: A probabilistic roadmap planner with sampling on the medial axis of the free space. In *IEEE Conference on Robotics and Automation*, 1999.

[25] Steven A. Wilmarth, Nancy M. Amato, and Peter F. Stiller. Motion planning for a rigid body using random networks on the medial axis of the free space. In *Proceedings of the 15th Annual ACM Symposium on Computational Geometry*, pages 173–180, June 1999.